Journal of Environmental Management 377 (2025) 124615

Contents lists available at ScienceDirect

Journal of Environmental Management

journal homepage: www.elsevier.com/locate/jenvman

Research article

Novel red mud waste-derived magnetic geopolymer spheres, made without the addition of any extra iron compounds, for the removal of wastewater contaminants

Tânia Gameiro [a,*], João Carvalheiras [a], Nuno P.F. Gonçalves [b], João S. Amaral [c], Robert C. Pullar [d], João A. Labrincha [a], Rui M. Novais [a]

[a] Department of Materials and Ceramic Engineering/ CICECO-Aveiro Institute of Materials, University of Aveiro, Campus Universitário de Santiago, 3810-193, Aveiro, Portugal
[b] Department of Chemistry/ CICECO-Aveiro Institute of Materials, University of Aveiro, Campus Universitário de Santiago, 3810-193, Aveiro, Portugal
[c] Department of Physics/ CICECO-Aveiro Institute of Materials, University of Aveiro, Campus Universitário de Santiago, 3810-193, Aveiro, Portugal
[d] Dipartimento di Scienze Molecolari e Nanosistemi (DSMN), Università Ca' Foscari Venezia, Via Torino 155, Venezia Mestre, 30172, Venezia (VE), Italy

ARTICLE INFO

Keywords:
Red mud-based geopolymer spheres
Thermal treatment
Iron reduction
Magnetic materials
Lead removal
Waste valorisation

ABSTRACT

In this work, and for the first time, the production of waste-based magnetic geopolymer spheres by a simple heat treatment under a reductive atmosphere is reported. Upon heat treatment, the iron oxide present in bauxite wastes (red mud), used as a solid precursor, is reduced to magnetite, thus producing magnetic spheres without the need for the addition of any secondary magnetic materials. The magnetisation of these mm-size materials reached 5.34 A m^2 kg^{-1}, suggesting they contain up to 6 wt% magnetite. This was demonstrated to be sufficient for their magnetic separation/removal, without the need for the addition of any extra magnetic iron oxides to the waste material. The magnetic spheres were then evaluated as sorbent materials for the removal of lead from water, selected as a model pollutant compound. These porous bulk-type sorbents showed high metal removal efficiency reaching an uptake value of 19 mg/g at pH 5 after 24 h of contact time. These promising results, and the easy post-treatment recovery of the waste-based magnetic spheres by the use of inexpensive permanent magnets, demonstrate the potential of the proposed strategy to address environmental concerns.

1. Introduction

Heavy metals, including lead, mercury, cadmium and arsenic, are naturally occurring elements that can become concentrated in the environment through industrial activities, mining, agriculture and improper waste disposal (Tan et al., 2020). These persistent and toxic metals pose serious risks to human health and the environment (Novais et al., 2020), degrading soil quality and impairing water quality, even at low concentrations (Tan et al., 2020). Lead has been widely used in various industries, resulting in widespread contamination of soil, water and air, with its presence being linked to immune system damage, liver issues and even cancer (Su et al., 2021).

Given the urgent need to reduce pollution, simple strategies for pollutant removal are preferred. Adsorption is a critical process in environmental remediation and water treatment, widely applied to remove heavy metals (Su et al., 2021), as well as dyes, pesticides, phosphorus and other pollution sources from water (Gameiro et al., 2023), due to its effectiveness, lower cost and simplicity (Tan et al., 2020). Several materials including activated carbon, zeolites and clay minerals such as bentonite and kaolinite have been considered sorbents, due to their high surface area and specific functional groups that facilitate the adsorption process (Gameiro et al., 2023). Geopolymers synthesised from aluminosilicate precursors using an alkaline activation process (Gameiro et al., 2021) have emerged as promising adsorbents for heavy metal removal from wastewater, due to their unique properties and environmental benefits (Novais et al., 2020; Novais and Labrincha, 2022). Geopolymer-based adsorbents can be produced from industrial by-products and wastes such as fly ash from biomass combustion, furnace slag or red mud (Alves et al., 2024), providing a sustainable solution for both waste valorisation and environmental remediation. Moreover, these types of sustainable materials can be tailored according to the wastewater characteristics and type of pollutant to be removed

* Corresponding author.
E-mail address: tania.gameiro@ua.pt (T. Gameiro).

https://doi.org/10.1016/j.jenvman.2025.124615
Received 22 October 2024; Received in revised form 23 January 2025; Accepted 16 February 2025
Available online 22 February 2025

(Salah et al., 2024), making them versatile and efficient for contaminant removal, particularly heavy metals.

Magnetic materials are advantageous due to their easy liquid/solid separation (El-Naggar et al., 2024) using magnetic fields, such as a permanent magnet (Rossatto et al., 2020), and subsequently the possibility of them being reused and recycled. The incorporation of magnetic properties into conventional geopolymers enables the recovery of the exhausted catalyst after an adsorption process (Tan et al., 2020). Also, the presence of iron improves the adsorption process since the number of active adsorption sites increases (Salah et al., 2024).

The incorporation of magnetic materials such as ferric oxide is a common methodology to improve the adsorption process and facilitate further adsorbent recovery steps. Magnetite (Maleki et al., 2019; Rossatto et al., 2020) and hematite (El-Naggar et al., 2024) are commonly added to the geopolymer composite to incur magnetic properties. However, this approach increases the cost of the process, such as for the chemical synthesis of magnetic zeolites (Su et al., 2023). Thermal treatment is an alternative procedure to obtain magnetic geopolymeric materials from iron-containing geopolymers. Geopolymers produced by using iron-containing precursors, such as red mud, already contain a considerable amount of hematite (Fe_2O_3) (Gonçalves et al., 2023). The thermal reduction of hematite can be triggered at high temperatures and under reducing conditions (hydrogen, nitrogen, carbon monoxide) to prevent oxidation reactions. This reduction follows three steps: Fe_2O_3 (hematite) → Fe_3O_4 (magnetite) → FeO (wüstite) → Fe (metallic iron) (Chen et al., 2020), resulting in metallic Fe if taken to completion. Magnetite is ferrimagnetic, and metallic iron is ferromagnetic. The occurrence of magnetite, wüstite or metallic iron is directly related to the reaction temperature (Pineau et al., 2006), and this can be used to tailor the magnetic properties of geopolymers. In a hydrogen atmosphere, the reduction of hematite starts at 160 °C and magnetite starts to appear. With an increase in temperature, magnetite starts to reduce, and metallic iron appears in the system. Wüstite should be formed at the same time as magnetite reduces, but the presence of this iron oxide mineral phase is normally detected above 580 °C (Stoicescu et al., 2022). For pure iron oxides, at temperatures higher than ≈600 °C, the reduction of magnetite is completed and metallic iron is the main iron-containing mineral phase (Pineau et al., 2006).

The high-temperature treatment for geopolymers can serve several purposes, namely the promotion of the growth of new crystalline phases within the geopolymer matrix, the induction of phase transformations and chemical reactions involving the precursor compounds, and the elimination of remaining water and organic compounds which lead to the densification and strengthening of the geopolymeric materials (Kuenzel et al., 2013; Padilla et al., 2022). The thermal conversion of iron-containing waste materials, such as red mud, through a reductive process, into new products with magnetic properties, without the need for any additional iron-containing additives, has a positive impact on environmental remediation and waste valorisation. This innovative approach is in line with the Sustainable Development Goals of the United Nations, which focus on the promotion of a circular economy through the reduction of natural resources consumption and, at the same time, the development of innovative solutions for complex wastes, such as red mud and fly ash, thus avoiding landfill deposition (Kumar et al., 2021). This valorisation strategy assumes vital importance since red mud, the by-product of alumina production from bauxite by the Bayer process, is considered a hazardous waste with high alkalinity and salinity (Kumar et al., 2021), with a global annual estimated production of 120 MT (Singh and Singh, 2019). The recycling and reusing of this challenging waste remain a large-scale problem, and its use in geopolymers production has been studied in recent years as a possible resolution. However, to date, the presence of iron oxide in wastes and geopolymer matrices has not been explored to obtain magnetic materials.

Most of the published works on magnetic geopolymers focus on the production of composites with added secondary magnetic phases, and their application as powder-type adsorbents. Maleki et al. achieved over 80% removal efficiency for heavy metals using a bentonite nanoclay-based geopolymer/Fe_3O_4 nanocomposite (Maleki et al., 2019), and El-Naggar et al. enhanced fly ash-based geopolymers with magnetic γ-Fe_2O_3 nanoparticles for effective removal of metals like Pb, Zn, and Cu (El-Naggar et al., 2024). Similarly, Su et al. used fly ash to create magnetic zeolite microspheres for cadmium removal (Su et al., 2023). Magnetic geopolymers have also shown excellent dye adsorption capabilities, with studies reporting high removal efficiency for dyes such as methylene blue (Al-husseiny and Ebrahim, 2022a), crystal violet (Salah et al., 2024), and others. Beyond adsorption, they have been applied in tetracycline removal (Al-husseiny and Ebrahim, 2022b) and even as heterogeneous catalysts for biodiesel production (Brandão et al., 2024), emphasising their versatility.

Magnetic geopolymeric adsorbents in powder form have been successfully applied to obtain high pollutant uptake; however, it requires a further separation step to recover the adsorbent material (Novais et al., 2020). To overcome this issue, this work presents for the first time the innovative production of bulk-type magnetic geopolymer spheres (mm-sized) through heat treatment in an inert atmosphere (N_2). The methodology reported here produced magnetic geopolymer spheres with inherent magnetic properties, without the need for any further magnetic additives. These properties enable straightforward recovery using a simple magnet, showing their potential for several applications. As a proof of concept, their use as adsorbents for heavy metal removal from wastewater, using lead as a pollutant model compound, was demonstrated. This highlights their dual functionality in adsorption and ease of recovery. This approach combines the benefits of geopolymer production with the versatility of magnetic materials, offering a sustainable solution for resource recovery and waste management practices.

2. Materials and methods

2.1. Materials

Red mud (RM), fly ash (FA) and metakaolin (MK) were used as aluminosilicate sources in the production of geopolymer spheres. RM is an iron-rich waste supplied as a slurry by an aluminium production industry. The slurry was dried at 100 °C, crushed and sieved to deagglomerate it. FA from biomass combustion was sieved, and particle sizes below 63 μm were used. Metakaolin (Argical™ M1200S, Univar) was incorporated into the composition to enhance the spheres' stability, also being were sieved below 63 μm to deagglomerate it.

The alkaline activator solution was prepared by mixing 100 g of sodium silicate solution (Chem-Lab) with 13.22 g of sodium hydroxide (97 % purity, Ercros) for 24 h following previous investigations (Gonçalves et al., 2024a).

2.2. Preparation of the magnetic spheres

2.2.1. Synthesis of the spheres

Geopolymer spheres were prepared using equal amounts (w/w) of RM, FA and MK (1:1:1), following the procedure described elsewhere (Gonçalves et al., 2024a). In detail, the alkaline activator solution was added to the blend of solid raw materials and mixed in a planetary mixer for 2 min. After that, 1.7 wt% sodium dodecyl sulphate (SDS, >99 %, Sigma) was added to the slurry as a foaming agent and mixed for 5 min. The foamed paste was used to prepare porous spheres by the suspension-solidification method (Alves et al., 2024). The paste was transferred to a syringe and injected dropwise in a polyethylene glycol (PEG 600, Alfa Aesar) medium at 80 °C. The spheres were removed from the consolidation medium (PEG) and washed with distilled water to remove excessive PEG and free alkalis within the structure (Tan et al., 2020). Initially, the spheres were cured at 40 °C for 24 h, followed by ambient curing conditions until the 28th day.

2.2.2. Production of the magnetic spheres

Geopolymer spheres obtained by the suspension-solidification method were heated at a heating rate of 10 °C/min to 400, 600 or 800 °C. The temperature was maintained for 2 h and a reductive atmosphere was created by nitrogen gas at 0.8 mL/min. These conditions (high temperature and reducing atmosphere) aimed to promote the reduction of hematite to magnetite, to obtain magnetic geopolymer spheres. Future studies will optimize the synthesis of magnetic spheres by refining reaction temperature, synthesis time, and reducing agent selection to enhance magnetic properties and reduce environmental impact. Fig. 1 presents a photograph of the produced magnetic materials heated to different temperatures.

2.3. Geopolymeric spheres characterisation

The physical-chemical properties of the spheres were evaluated after curing for 28 days. The chemical composition was obtained by X-ray fluorescence spectroscopy (Philips X'Pert PRO MPD spectrometer). The mineralogical composition was evaluated by X-ray diffraction (XRD) in a Panalytical X'Pert Pro3 diffractometer (Cu K_α radiation, 10–80° 2θ, 0.02 2θ step-scan, 10 s per step) and the phase identification was performed with Panalytical X'Pert HighScore Plus software. The apparent density of the bulk spheres was measured using a helium pycnometer (Anton Paar, ultrapyc 500 micro). The specific surface area (SSA) was measured using nitrogen adsorption via the multi-point Braunauer-Emmet-Teller (BET) method, performed with a Micromeritics Gemini 2380 analyser.

The relationship between the mass change and heat treatment temperature of the spheres was studied by thermal analyses on a Hitachi STA300 instrument, working under an air atmosphere. The weight losses were performed by heating ca. 8–10 mg of each sample by applying a heating ramp from 30 to 800 °C (rate 10 °C/min). The microstructure of the spheres, before and after heat treatment, was evaluated in samples coated with carbon using scanning electron microscopy (SEM – Hitachi SU-70) equipped with energy dispersion spectroscopy (EDS – Bruker Quantax 400). Fourier-transform infrared spectroscopy (FTIR) measurements were performed to evaluate the molecular bonds of the geopolymer spheres. FTIR spectra were collected using a Bruker Optics Tensor 27 spectrometer coupled to a horizontal attenuated total reflectance (ATR) Golden Gate cell (Specac), using 256 scans at a resolution of 4 cm^{-1}. The magnetic properties of the spheres were evaluated using a superconducting quantum interference device (SQUID, Quantum Design MPMS3) magnetometer at 300 K with applied magnetic fields up to 1 T.

2.4. Removal of lead as a proof of concept

The adsorption capacity of a selected composition was evaluated using a synthetic solution of lead as a model pollutant. Adsorption was tested in batch mode, in a total volume of 50 mL of lead solution and a solid-to-liquid ratio of 4. For these tests, spheres treated at 600 °C were chosen due to their higher saturation magnetisation (see discussion in section 3.2.5) and, thus, with potential to be further recovered by a simple magnet. The samples were kept under magnetic stirring (without a magnetic stirring bar) and the tests were performed in triplicate. The effects of pH (3, 4 and 5), initial lead concentration (50, 100 and 200 ppm) and contact time (up to 24 h) were evaluated to estimate the adsorption performance of the magnetic spheres. In the adsorption assays evaluating the influence of pH, the initial pH of the synthetic lead solution was adjusted to 2, 3 or 4 and maintained constantly throughout the experiment by manually adding HNO_3 (0.05 M) as needed. This pH control was used to prevent lead precipitation, which can occur at higher pH values (Gonçalves et al., 2024b).

The Pb quantification was performed by a Total reflection X-ray fluorescence spectrometer (TXRF – S2 PICOFOX 50 keV), with a detection limit in the ppb range. The pH measurement was performed using a Thermo Scientific Orion Star A211.

3. Results and discussion

3.1. Characterisation of raw materials

Before being used as raw materials in the spheres' production, RM, FA and MK were characterised. The chemical composition of the raw materials (see Table 1) estimated by XRF revealed a noteworthy higher content of iron oxide in RM (48 wt%) compared with FA (6 wt%) and MK (2 wt%), as well as greater Na_2O and TiO_2 content in RM. On the contrary, SiO_2 content in FA (50 wt%) and MK (52 wt%) was much higher than that seen in RM (6 wt%), and a similar trend was observed for Al_2O_3.

The mineralogical composition of raw materials was determined by XRD, and the results are presented in Fig. 2. The XRD pattern of RM shows the presence of hematite (α-Fe_2O_3) and aluminium-bearing hydroxide phases including boehmite (γ-AlO(OH)), chantalite ($CaAl_2SiO_4(OH)_4$) and gibbsite (α-$Al(OH)_3$). The XRD patterns of FA and MK show the presence of Si-based crystalline phases, such as quartz (SiO_2) and muscovite ($KAl_3Si_3O_{10}(OH)_{1.8}F_{0.2}$), as well as anatase ($TiO_2$).

3.2. Characterisation of geopolymer spheres

3.2.1. Morphological analysis (SEM) and chemical composition

Figs. 3 and 4 present SEM micrographs of the geopolymer spheres, before and after the thermal treatment. Before the thermal treatment (Figs. 3a and 4a), the exterior surface of the spheres shows the presence of small pores combined with larger-sized pores, while the inner part shows an abundant number of pores, mostly closed.

It can be observed that the temperature seems to influence the porosity of the spheres, with a significant modification of the spheres' external surface at higher temperatures. Spheres exposed to thermal treatment at 800 °C (Fig. 3d) present a higher number of pores at the external surface compared to those without treatment (Fig. 3a), or even

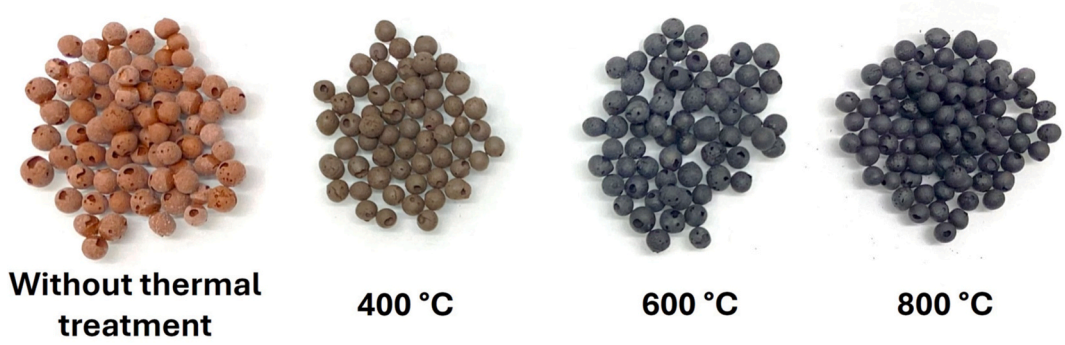

Fig. 1. – Geopolymer spheres obtained without thermal treatment and after thermal treatment at different temperatures (400, 600 and 800 °C).

Table 1
– Chemical composition of the raw materials (RM, FA and MK) and the geopolymer spheres estimated by XRF. Loss on ignition (LOI) was determined at 1100 °C.

Oxides (%)	SiO_2	Al_2O_3	Fe_2O_3	TiO_2	MgO	Na_2O	CaO	MnO	K_2O	SO_3	P_2O_5	LOI
RM	6.30	19.20	48.40	6.67	0.08	5.77	1.10	0.05	0.07	0.22	0.36	11.00
FA	42.72	13.66	5.78	0.81	2.79	1.27	18.74	0.35	6.41	2.53	1.44	2.68
MK	52.10	40.10	1.85	1.70	0.27	0.08	0.13	0.01	1.09	0.04	0.07	2.24
Geopolymer spheres	32.90	15.73	11.11	1.92	0.49	11.44	3.83	0.08	1.28	0.52	0.34	20.03

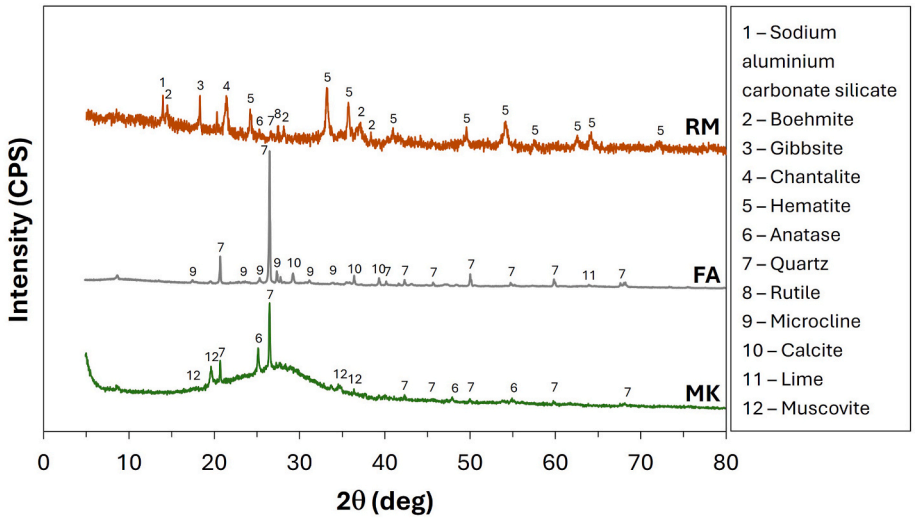

Fig. 2. – XRD patterns of the raw materials (RM, FA and MK).

those at lower temperatures such as 400 °C (Fig. 3b). These variations are also visible in the inner part, with a significant modification of the porosity of the specimen after 2h at 800 °C (Fig. 4d), when compared to spheres obtained at 600 °C (Fig. 4c) and at 400 °C (Fig. 4b). The formation of small pores throughout the spheres' surface treated at higher temperatures is related to both water evaporation and the material's partial transformation, from amorphous geopolymer spheres to crystalline materials (Kljajević et al., 2022). This transformation was also observed by other authors (Kljajević et al., 2017; Kuenzel et al., 2013; Payakaniti et al., 2020), who reported the formation of porous geopolymer materials after thermal treatments at temperatures above 600–800 °C. The pore formation at high temperatures is also related to the reduction reactions of iron oxides and carbonates, releasing oxygen (O_2) or carbon dioxide (CO_2), which become trapped within the geopolymer matrix and can lead to the formation of voids or pores (Kljajević et al., 2022).

With the increase of treatment temperature, a slight increase in the apparent density of the spheres was observed, from 2.2 g/cm^3 (initial geopolymer spheres) to 2.7 g/cm^3 (geopolymer spheres treated at 600 °C) and 2.8 g/cm^3 (geopolymer spheres treated at 800 °C), as also referred by other authors (Zawrah et al., 2022). These changes can be related to the phase transformations observed in spheres with thermal treatment.

A decrease in the specific surface area (SSA) of the geopolymer spheres was observed following thermal treatment. The initial spheres exhibited an SSA of 34 m^2/g (Gonçalves et al., 2024a), which reduced to 20 m^2/g after treatment at 600 °C and further decreased to 4 m^2/g at 800 °C. Despite this reduction, the SSA of the magnetic spheres treated at 600 °C remains slightly higher than the values reported for geopolymer adsorbents produced via additive manufacture using metakaolin as the aluminosilicate source. For instance, Luukkonen et al. reported an SSA of 6.0 m^2/g (Luukkonen et al., 2020), while Franchin et al. obtained an SSA of 12.2 m^2/g (Franchin et al., 2020). The reduction of SSA reflects the progressive densification of the material as the temperature increases. The pore volume of the geopolymeric material followed a similar trend, decreasing from 0.075 cm^3/g to 0.045 cm^3/g after the thermal treatment at 600 °C and further dropping significantly to 0.010 cm^3/g at 800 °C.

The EDS maps of the cross-section of the geopolymer spheres before and after thermal treatment are presented in Fig. 5. The EDS analysis of the external surface of the geopolymer spheres before thermal treatment revealed the presence of the characteristic elements of the raw materials and alkaline activator, namely Al, Si, Na, K, Ti and Fe, in line with our previous studies (Alves et al., 2024; Gonçalves et al., 2024a). The presence of iron was detected uniformly throughout the interior of the geopolymer spheres, and it can be related to the increase in the magnetisation of the samples, observed using a magnet. Other elements such as Al, Si, Na, Ca, K and Ti were also detected and are the basis of the geopolymeric spheres' composition, and quantities were similar to the total chemical compositions of the solid raw materials used to produce the spheres, namely RM, FA and MK.

The chemical composition of the geopolymer spheres was estimated by XRF, and the results are included in Table 1. XRF analysis revealed the presence of high contents of SiO_2 (33 wt%), Al_2O_3 (16 wt%), Na_2O (11 wt%) and Fe_2O_3 (11 wt%). These elements were previously detected in the chemical composition of the precursors (RM, FA and MK) at high levels, and are in line with the results obtained in the EDS analysis. Considering the composition of the geopolymer spheres, namely a 1:1:1 ratio of the solid precursors and 45 wt% of alkaline activator added to the paste mixture, the theoretically estimated amount of each oxide and the values obtained by XRF were similar (estimated difference of ≈5 %). The high contents of SiO_2 and Na_2O are related to the nature of the alkaline activator, a mixture of sodium silicate and sodium hydroxide.

3.2.2. XRD

The XRD patterns obtained for the geopolymer spheres before and after the thermal treatment at different temperatures are presented in Fig. 6. The non-treated spheres show the characteristic amorphous halo in the range of 2θ° = 20–35°, which was attenuated in the heat-treated samples due to the formation of new crystalline phases and reduction of

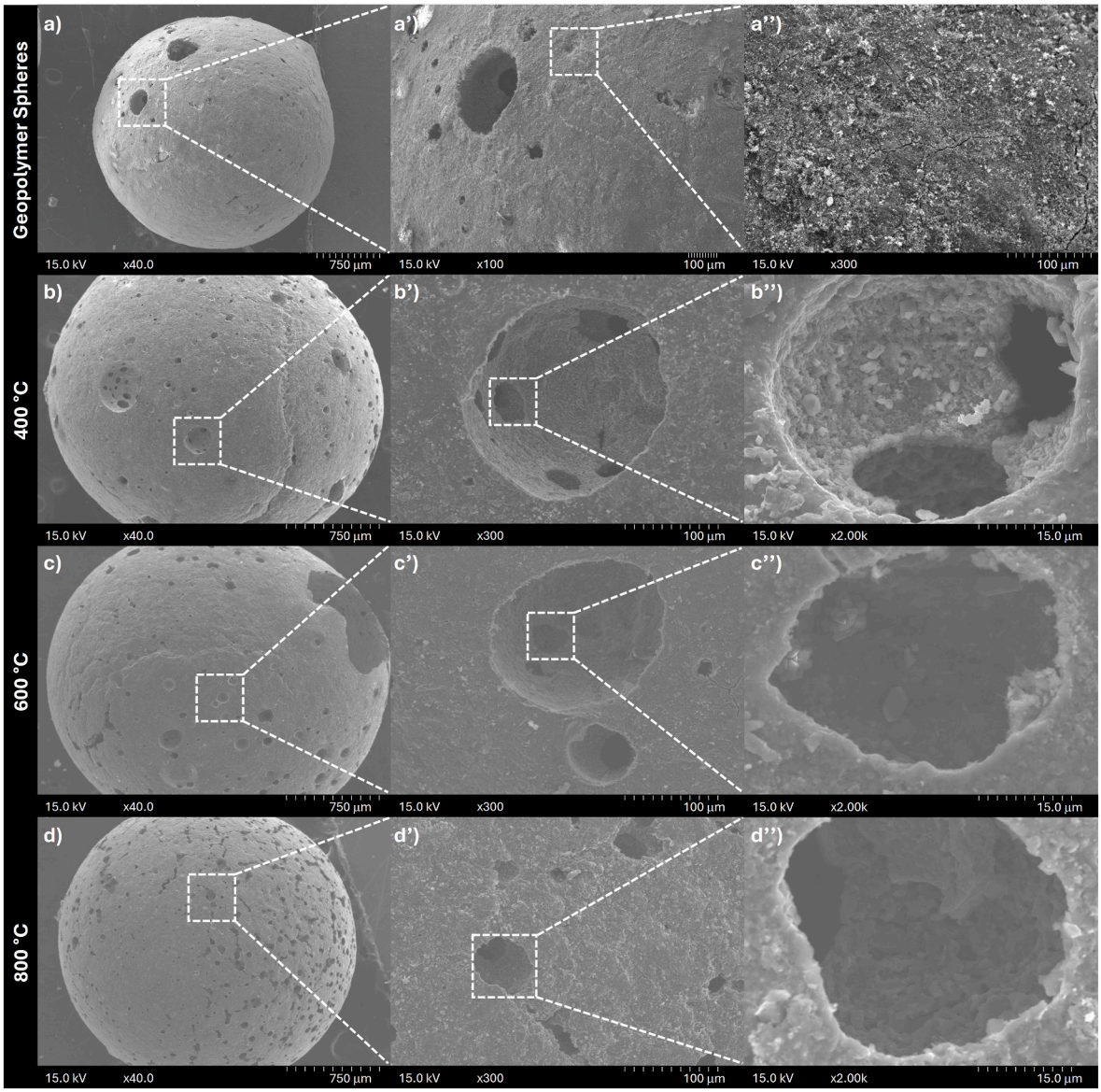

Fig. 3. – SEM micrographs of the geopolymer spheres' surface before (a) and after thermal treatment at 400 °C (b), 600 °C (c) and 800 °C (d).

the amorphous content (Payakaniti et al., 2020). For the samples treated at 800 °C, the amorphous halo disappears, and new reflections are visible. The crystalline mineral phases identified in the sample without thermal treatment and with thermal treatment at 400 °C were similar, which is indicative of the thermal stability of the geopolymer spheres up to 400 °C (Moutaoukil et al., 2024). However, changes were observed in the diffraction patterns with the increase of the temperature to 600 °C and 800 °C. The intensity of the quartz reflections decreased in the sample treated at 800 °C, and was related to the conversion of α-quartz to β-quartz at temperatures above 573 °C (Kljajević et al., 2022). This behaviour was also observed by other authors (Kljajević et al., 2017; Payakaniti et al., 2020).

Magnetite appeared after the thermal treatment at 400 °C, suggesting the reduction of iron-containing phases such as hematite, initially present in the non-modified geopolymer spheres. Raising the temperature increased the intensity of the peaks assigned to magnetite (main peaks at 35.58, 62.82 and 43.25 2θ°) and this variation was clear when the heat treatment temperature increased from 400 to 600 °C, demonstrating that high temperatures favour the formation of magnetite through the reduction of iron(III) oxides. Hematite (α-Fe_2O_3) containing only Fe^{3+} is known to be able to convert to ferrimagnetic magnetite (Fe_3O_4) under suitable conditions, containing both Fe^{3+} and Fe^{2+}. For the reductive atmosphere here studied (N_2), the reduction profile of iron oxides present in the geopolymer spheres was similar to that described by Stoicescu et al. for magnetite particles (Stoicescu et al., 2022) and by Pineau et al. for synthetic hematite (Pineau et al., 2006), studies that used hydrogen and nitrogen atmospheres, respectively.

Hydroxide-containing phases such as chantalite, gibbsite and boehmite were not identified with an increase in the thermal treatment temperature. When gibbsite is heated to 250 °C water is released and, simultaneously, boehmite is formed as an intermediate product in temperature ranges of 350–450 °C (Riyanto et al., 2021). The dehydration and decomposition of boehmite occurs at even higher temperatures, and it explains the presence of boehmite in the samples treated at 400 °C and its absence in the samples treated at 600 °C and 800 °C. Calcite ($CaCO_3$) thermally decomposes above 750 °C (Karunadasa et al., 2019), and it explains the absence of this calcium-containing phase in the sample treated at 800 °C.

The XRD pattern of the sample treated at 800 °C is significantly different from the other samples, indicating considerable transformations in the arrangement of atoms. The reducing environment applied during the thermal treatment boosted the further removal of

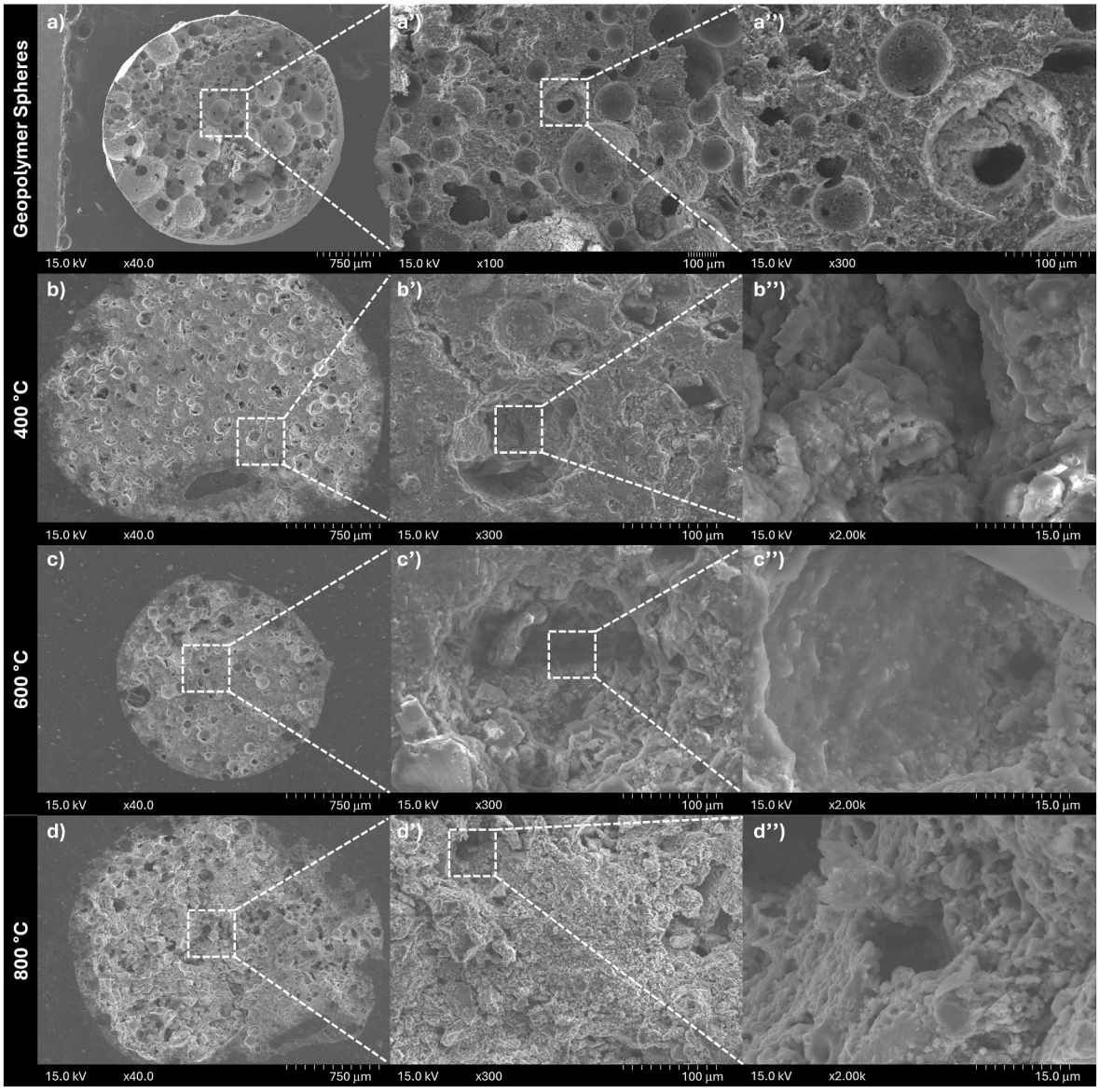

Fig. 4. – SEM micrographs of the geopolymer spheres' interior before (a) and after thermal treatment at 400 °C (b), 600 °C (c) and 800 °C (d).

oxygen atoms from magnetite, resulting in an at least partial reduction to metallic α-iron, whose main peaks (44.67 and 65.02 2θ°) appeared in the XRD patterns at 800 °C. Other authors also reported the full reduction of magnetite to metallic iron at temperatures above 600 °C in a reductive atmosphere, starting from commercial hematite (Pineau et al., 2006). The appearance of nepheline ($Na_3KAl_4Si_4O_{16}$) as the main crystalline phase was also induced by high temperature (800 °C), and this occurrence was reported previously (Kljajević et al., 2017) for heated-treated geopolymers. The formation of nepheline, a type of feldspathoid mineral, is a complex process that involves chemical, structural and mineralogical changes, probably caused by the migration and/or the ejection of atoms from the crystal lattice of the geopolymer spheres, which led to variations of chemical stoichiometry and expansion or contraction of the material (Padilla et al., 2022). The high temperatures promote the crystallisation of nepheline within the geopolymer matrix, where the sodium ions from the alkaline activator react with aluminosilicate structures to form nepheline (Kljajević et al., 2017). Ilmenite ($FeTiO_3$) and Hedenbergite ($CaFeSi_2O_6$) were also found in the XRD patterns of the geopolymer spheres treated at 800 °C. The formation of these calcium, iron and titanium-bearing crystalline phases was favoured at high temperatures.

3.2.3. FTIR

The infrared spectra of the geopolymer spheres obtained by ATR-FTIR spectroscopy are presented in Fig. 7a. In the spheres without thermal treatment, the characteristic bands of the raw materials (data not shown here for the sake of brevity, details can be found in (Gonçalves et al., 2024a)) are also present, namely the asymmetric band located between 1150 and 950 cm^{-1} due to the presence of Si and Al ions from the aluminosilicate precursors (RM, FA and MK). Also, another wide asymmetric band with a maximum at 3360 cm^{-1} is present in the spheres without thermal treatment and in the precursors (mainly RM), due to the presence of physically adsorbed molecular H_2O on the surface (Gameiro et al., 2023), which also results in a small band around 1650 cm^{-1} rising from the H-O-H bending vibrations (Mullaimalar et al., 2024). A blue shift in the Si-O-Al/Si-O-Si band with a peak at 970 cm^{-1} was observed in the geopolymer spheres relative to the precursors, and it is usually associated with the geopolymerisation reaction (Luukkonen, 2022; Phokha et al., 2023). The band with a peak at 1450 cm^{-1} is related to the asymmetric stretching of carbonate ions (Payakaniti et al., 2020), mainly due to the presence of calcite (Gonçalves et al., 2023), as confirmed by the XRD patterns. In all samples, the noise observed in the region between 2380 and 1930 cm^{-1} is due to atmospheric CO_2

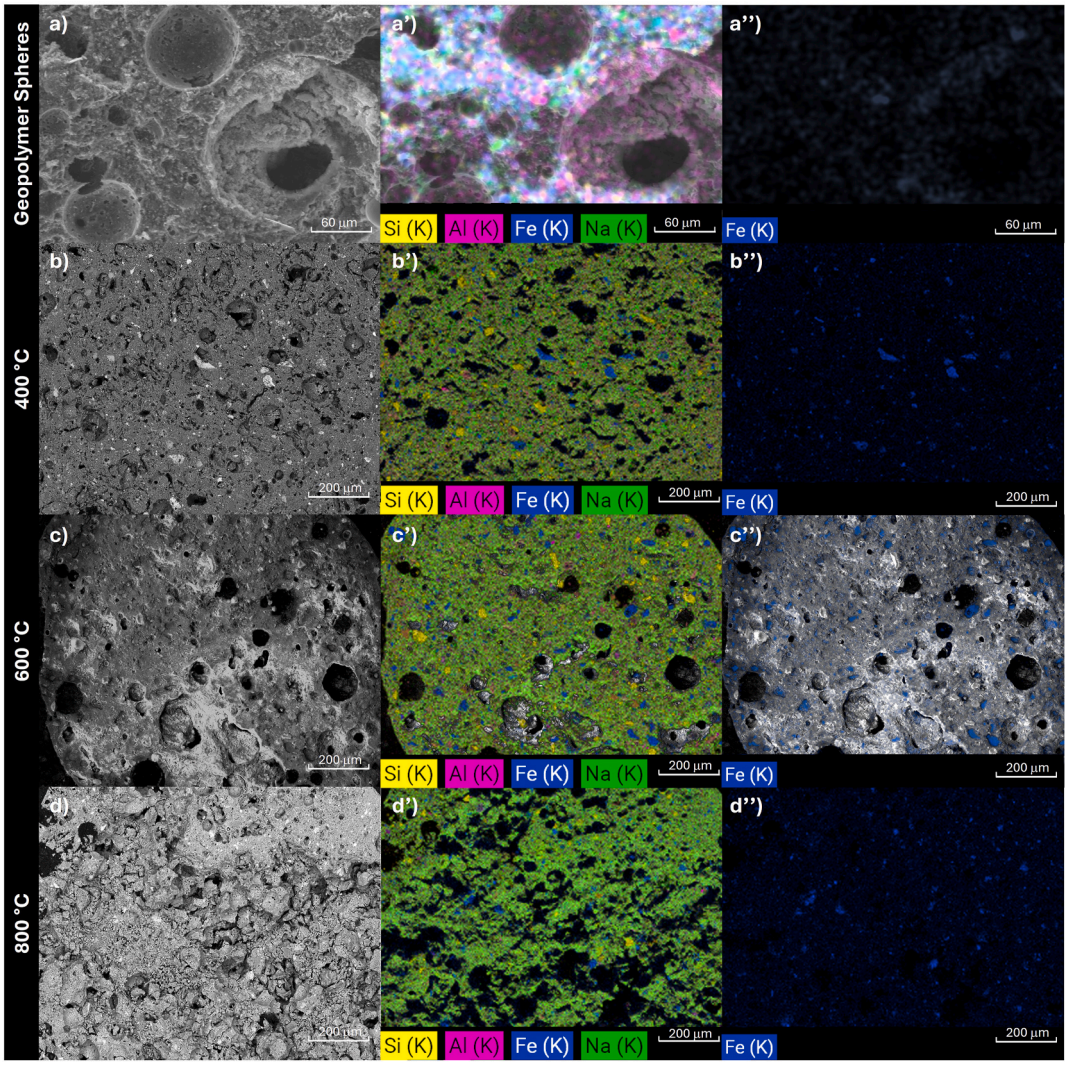

Fig. 5. – EDS maps of the geopolymeric spheres' interior before (a) and after thermal treatment at 400 °C (b), 600 °C (c) and 800 °C (d).

(Gonçalves et al., 2023).

With the thermal treatment of geopolymer spheres, the peaks present lower intensities due to the breakage of bonds and the formation of new phases (Payakaniti et al., 2020), consistent with the XRD results. A decrease in the intensity of bands with maxima of ≈3400 and 1600 cm^{-1} was observed, as a function of the temperature, indicating full dehydration of the geopolymers (Salah et al., 2024). The small band with a peak at 1450 cm^{-1} presents a similar trend, due to a decrease in the carbonatate content for the samples with thermal treatment at greater temperatures. At high temperatures, the carbonate compounds decompose and start to react with the silica and alumina released from gels to form other mineral compounds, such as nepheline (Ahmad et al., 2021), as observed in the XRD patterns. Additionally, exposing geopolymers to higher temperatures also promotes a decrease in the intensity of the band with a maximum at 970 cm^{-1}, corresponding to the asymmetric stretching of Al-O-Al/Si-O-Si (Luukkonen, 2022), and this can be explained by the polymeric structural reorganisation and the changes in the crystalline phases' composition.

The increase in the definition of the band with a peak at ≈ 680 cm^{-1}, corresponding to the Si-O-Al functional group (Gonçalves et al., 2023), was observed with the increase in the treatment temperature. A similar transformation with the increase in temperature was also observed by other authors (Payakaniti et al., 2020). The peaks located at 440 cm^{-1} can be attributed to the stretching of the Fe-O bond of the hematite phase (Gonçalves et al., 2023). The increase in the definition of the peak with the increase in temperature can be explained by the changes in the iron-containing phases (Su et al., 2023), with the conversion of hematite into magnetite, as discussed in the previous section.

3.2.4. *Thermogravimetric analysis (TGA)*

Changes in the mass of the geopolymer spheres as a function of temperature under a controlled atmosphere were determined using TGA. The TGA curves obtained are presented in Fig. 7b. The mass of geopolymer spheres without thermal treatment rapidly decreased between room temperature and 180 °C (≈13.9 %), due to water loss. This process is associated with the loss of adsorbed free water and with the bound water from some hydrated phases (Moutaoukil et al., 2024). These geopolymer spheres also presented a mass loss between 200 °C and 500 °C (≈15.9 %), due to the dehydroxylation of chemically bound water from the matrix (Moutaoukil et al., 2024) and the breakdown of hydroxyl groups from the aluminosilicate gel network (Tchakouté et al., 2017). In this temperature range, gibbsite and boehmite also decompose, and these changes in the geopolymer crystalline composition contributed to the mass loss (Riyanto et al., 2021). Also, the remaining PEG within the spheres is decomposed in a single step, and this decomposition reaction further contributed to the mass decrease within the range of 300–400 °C (Alves et al., 2024). A third significant thermal degradation occurred above 500 °C (≈2.5 %), and this weight loss was attributed to the decomposition of carbonates (Maleki et al., 2019; Pulidori et al., 2024) and further loss of oxygen upon the reduction of

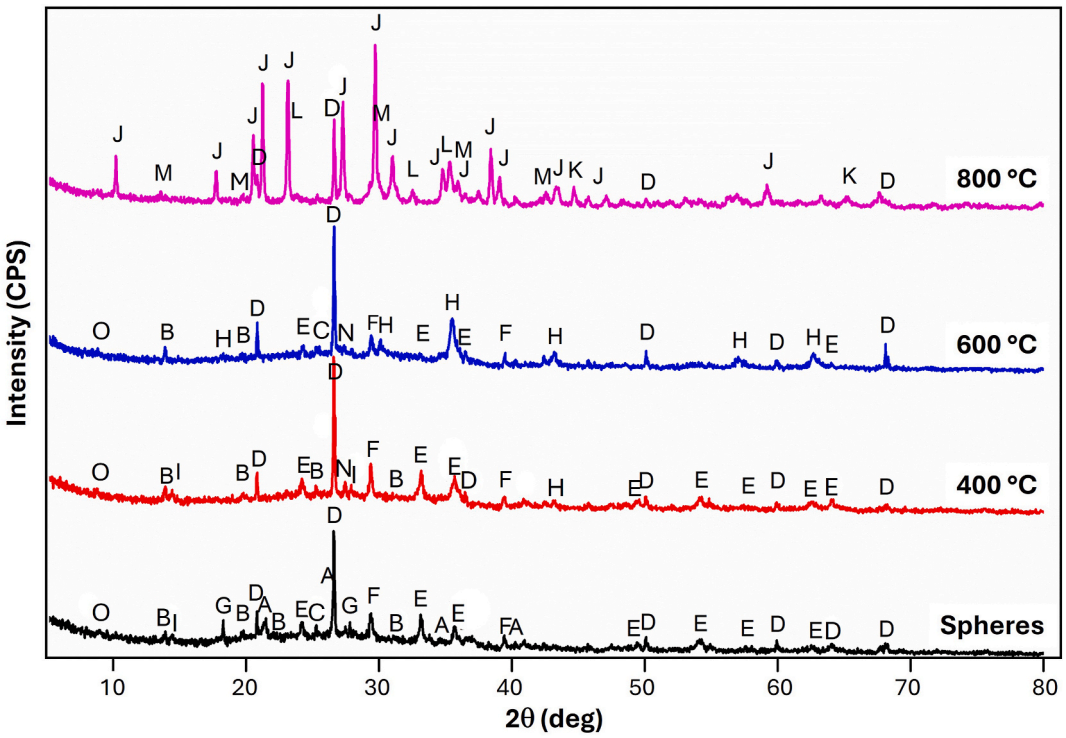

Fig. 6. – XRD patterns of the geopolymer spheres before and after thermal treatment at 400, 600 and 800 °C. A – Chantalite; B – Sodium aluminium silicon carbonate oxide; C – Anatase; D – Quartz; E – Hematite; F – Calcite; G – Gibbsite; H – Magnetite; I – Boehmite; J – Nepheline; K – Metallic α-Iron; L – Ilmenite; M – Hedenbergite; N – Rutile; O – Annite.

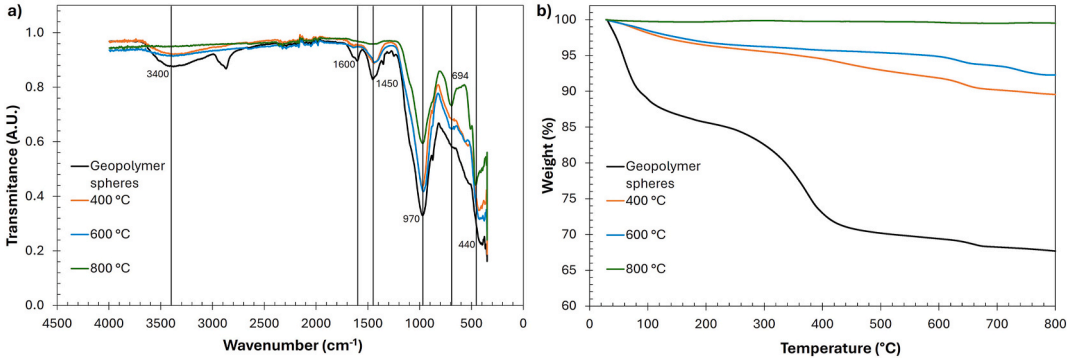

Fig. 7. – a) ATR-FTIR transmittance spectra and b) TGA curves of geopolymer spheres without and with thermal treatment at different temperatures.

iron oxides, namely hematite to magnetite (Kljajević et al., 2022).

As expected, the TGA curves of the heat-treated samples were significantly different from the curves obtained for the non-modified geopolymer spheres. The overall mass loss decreased drastically with the increase of the treatment temperature: 10.5, 7.7 and 0.5 % mass loss for the geopolymer spheres treated at 400, 600 and 800 °C, respectively. The almost null weight loss observed for samples treated at 800 °C reveals the complete decomposition of volatile components (water and carbonates) and the formation of stable crystalline phases at this temperature.

3.2.5. *Magnetic properties*

The geopolymer spheres produced throughout the thermal treatment at different temperatures presented an observable magnetism, as all fired samples were attracted to a magnet, as can be seen in Fig. 8.

Fig. 9a presents the measured specific mass magnetisation *M* versus the applied magnetic field of all the samples, measured at 300 K. Not surprisingly, the *as-produced* spheres did not have any significant magnetic properties, as they do not contain any strongly ferromagnetic/ferrimagnetic phases, contrasting with those submitted to the heating protocol. After heating, the samples all exhibited magnetic hysteresis loops, the magnetisation of the spheres increasing with the increase of the applied magnetic field (Su et al., 2023), although none were fully saturated up to a field of 1 T. At the maximum magnetic field of 1 T the mass magnetisation value of the samples (M) was evaluated, and the results are presented in Fig. 9b. The values of magnetisation M at 1 T, remanent magnetisation M_r and coercivity H_c are shown in Table 2 for all samples.

The untreated spheres only contain hematite as an iron oxide phase, and this is only very weakly ferromagnetic (or a canted antiferromagnet) at 300 K (Cornell and Schwertmann, 2006). As a result, they had an extremely low magnetisation of 0.15 A m^2 kg^{-1}, as well as a low coercivity H_C and remanent magnetisation M_r (Table 2). Thermally treated samples showed well-defined hysteresis loops characteristic of ferrimagnetic behaviour due to the presence of magnetite (Payakaniti et al., 2020). A major increase in M was observed when the heating

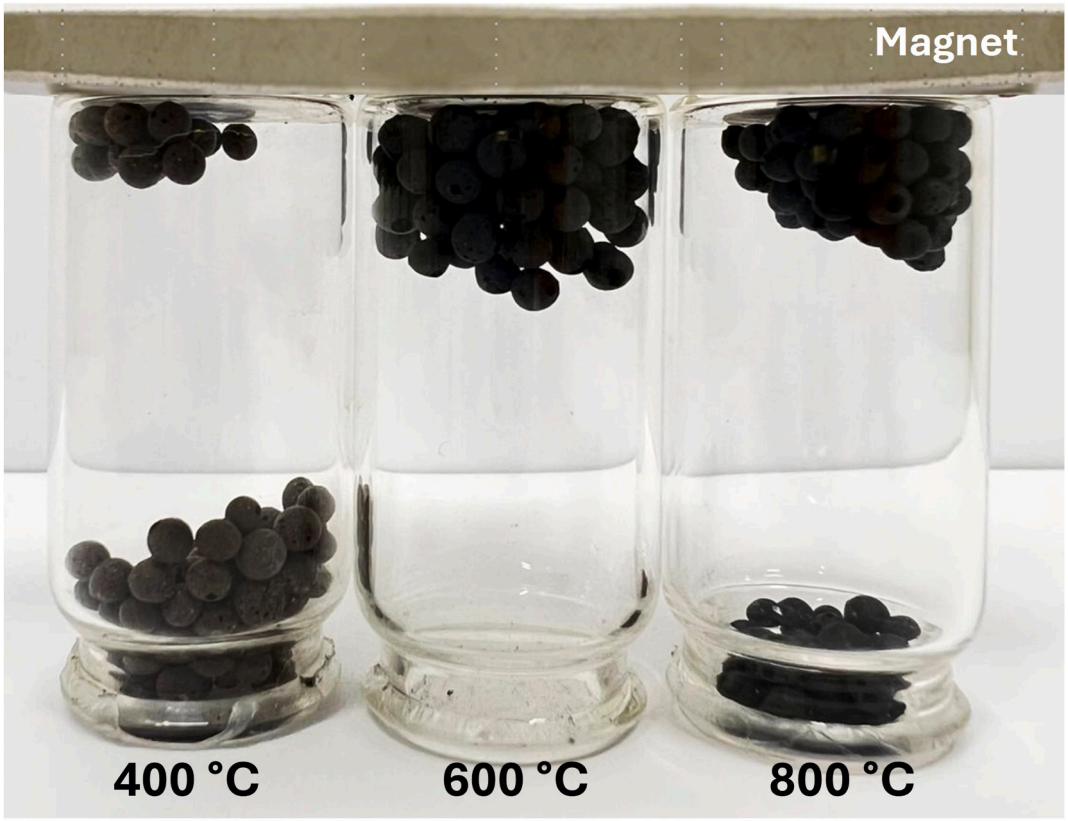

Fig. 8. – Attraction of samples heated to 400, 600 and 800 °C to a magnet.

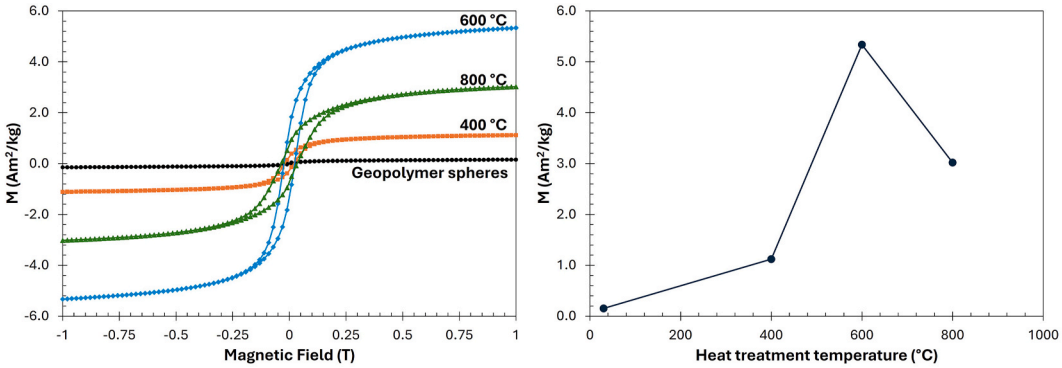

Fig. 9. – a) Magnetisation curves of geopolymer spheres before and after thermal treatment, measured at 300 K; b) Mass magnetisation (M) of the geopolymer spheres, measured at an applied field of 1 T and 300 K, as a function of processing temperature.

Table 2
– M at 1 T, M_r and H_c of the samples without and with thermal treatment, determined at room temperature.

	M (A m^2 kg^{-1})	M_r (A m^2 kg^{-1})	H_c (A m^{-1})
Spheres without thermal treatment	0.15	0.02	100
Spheres with thermal treatment at 400 °C	1.12	0.26	197
Spheres with thermal treatment at 600 °C	5.34	1.34	240
Spheres with thermal treatment at 800 °C	3.02	0.73	350

temperature increased from 400 °C (1.12 A m^2 kg^{-1}) to 600 °C (5.34 A m^2 kg^{-1}). This suggests that significantly more magnetite was present after heating to 600 °C. Indeed, this can be directly correlated with the amount of magnetite identified by XRD analysis (see section 3.1.3). However, the actual maximum M measured here of 5.34 A m^2 kg^{-1}, compared to usual values for pure magnetite of around 90 A m^2 kg^{-1} (Ben-Arfa et al., 2019; Cornell and Schwertmann, 2006), suggests that the spheres still only consist of around 6 wt% magnetite. This is consistent with the fact that hematite is also still detectable in the XRD patterns after treatment at 600 °C, and XRF showed that the maximum Fe_2O_3 content was around 11 wt%, so not all hematite was reduced to magnetite. Nevertheless, this is still a significant magnetisation and was demonstrated to be enough to allow for the magnetic separation/removal of the spheres, without adding any extra iron oxides to the existing waste material. All of the magnetic loops portrayed quite magnetically soft materials, with narrow hysteresis loops and low H_c and

M_r values, as expected for magnetite. H_c was only around 200–240 A m^{-1} for the spheres heated at 400–600 °C, with M_r values around 25% of M measured at 1 T.

Higher treatment temperatures (>600 °C) led to a decline in the samples' magnetisation to 3.02 A m^2 kg^{-1}, as XRD showed the apparent loss of the magnetite phase, to be replaced by a much smaller quantity of metallic iron, as well as the non-magnetic mineral phase Hedenbergite ($CaFeSi_2O_6$). When heated to 800 °C, M_r as a % of M remained similar, but there was a small increase in the magnitude of the coercivity to H_c = 350 A m^{-1}, probably due to the formation of metallic α-Fe. Therefore, magnetite has been further reduced to partially form metallic iron, with the rest of the Fe incorporated into Hedenbergite. Although α-Fe has a greater magnetisation that magnetite, there was much less of it present, so the magnetisation of the spheres was reduced after heating to 800 °C. These results demonstrate that the proposed approach leads to the production of geopolymer spheres with suitable magnetic properties endowing their easy magnetic recovery after wastewater treatment.

The values obtained for M of the geopolymer spheres with thermal treatment were in the same range reported by several authors, who describe the production of magnetic geopolymers. The addition of magnetite (Rossatto et al., 2020) or hematite (El-Naggar et al., 2024) sources is the most common approach to obtaining magnetic geopolymers, and results for M_{sat} obtained by several authors are summarised in Table 3. For comparison, the M value of pure magnetite (90 A m^2 kg^{-1}) (Ben-Arfa et al., 2019; Cornell and Schwertmann, 2006) was also included in the table.

The incorporation of magnetic sources in the geopolymer composites generally resulted in M values between 2.50 and 4.95 A m^2 kg^{-1}, below the values obtained in this study for the geopolymer spheres treated at 600 °C (5.34 A m^2 kg^{-1} g). Considering the nature of the waste-based geopolymer spheres, with the incorporation of fly ash and red mud in the composition, the M values obtained are promising, and the use and recovery of these materials are enhanced due to the tailored magnetic properties.

3.3. Application of magnetic geopolymer spheres as metal sorbents

3.3.1. Adsorption tests: effect of pH

The adsorption potential of red mud-based geopolymeric materials has been demonstrated in several published works. Carvalheiras et al. tested highly porous monoliths for led removal, evaluating the influence of contact time, pollutant concentration, pH of the synthetic solution and solid-to-liquid ratio (Carvalheiras et al., 2023). The adsorption potential of red mud-based geopolymer spheres was tested by Gonçalves et al. to treat acid mine drainage waters, highlighting the interesting removal efficiency of these innovative geopolymeric materials and ability to treat complex wastewater streams (Gonçalves et al., 2024a).

Considering that the highest magnetisation was seen for the spheres fired at 600 °C, the potential of the materials obtained in the present work to act as metal sorbents from polluted waters was evaluated, using lead as a pollutant probe. The adsorption tests presented act as a proof-of-concept to demonstrate the applicability of these magnetic materials in addressing a highly relevant environmental challenge.

As detailed in section 2.4, batch adsorption experiments were performed by keeping the porous magnetic spheres under continuous stirring without the need for a magnetic stirring bar. The impact of the solution pH on the removal efficiency is presented in Fig. 10a. For all investigated pH conditions, a fast removal was observed within the initial 8 h of contact time, followed by a minor gain up to 24 h. The fast removal efficiency in the initial stage is explained by the high amount of available adsorption sites in the adsorbent (geopolymer spheres), which gradually become occupied over time (Gameiro et al., 2023). In the first 2 h of contact time, 20 % removal was observed at lower pH, while similar removal efficiency percentages (≈37 %) were seen for pH 4 and 5. Nonetheless, longer contact time resulted in superior pollutant removal at pH 5. Indeed, the pH of the medium strongly impacted the removal efficiency for the pollutant by the porous geopolymer spheres, with it jumping from 52 % at pH 3–77 % at pH 5, after 24 h. However, the additional contact time between 8 and 24 h had promoted an increment of only 12 % and 8 % for the tests at pH 4 and pH 5, respectively. In this case, the increase in contact time may represent an additional operational cost when considering a full-scale application, without a significant improvement in the process performance.

An increment in the pH of the medium favoured not only the removal efficiency, but also the uptake, which increased by 64 % at pH 5 compared with pH 3, as shown in Fig. 10b. Uptake values reached a maximum at pH 5, achieving 10.2 mg/g. This performance is superior to the work of Novais et al. with porous biomass fly ash-containing geopolymer monoliths, which achieved a maximum uptake value of 6.34 mg/g at pH 5 (Novais et al., 2016a).

3.3.2. Adsorption tests: effect of initial pollutant load

Fig. 11a and b presents the influence of the lead initial concentration on removal efficiency and uptake, respectively. For these tests, performed at pH 5, a similar trend was observed: a fast removal within the initial 8 h followed by a minor increase until the end of the experiment. This behaviour was observed for all investigated Pb concentrations. Moreover, the initial lead concentration influenced the efficiency removal, as it decreased with the increase of initial concentration from 50 to 200 ppm. The 77 % removal efficiency observed for assays at the initial concentration of 50 ppm declined to 38 % at 200 ppm of Pb, after 24 h of contact time. This behaviour suggests the saturation of the available sorbent active sites for higher investigated concentrations (Gameiro et al., 2023). This is in line with the reported studies using geopolymer monoliths (Carvalheiras et al., 2023), fly-ash based geopolymer foams (Caetano et al., 2022) and 3D-printed geopolymers (Gonçalves et al., 2023) for water borne pollutants removal.

Contrary to the observed behaviour of removal efficiency, raising the initial metal concentration led to an increase in the uptake values. The increase in the initial metal concentration provides the necessary driving force and concentration gradient to enhance the adsorption capacity, thus increasing the uptake. Increasing the initial metal concentration from 50 to 100 and 200 ppm resulted in an uptake increase from 10 mg/g to 14 mg/g and 19 mg/g, respectively. Although the values achieved for 200 ppm were slightly lower than those reported in the literature, similar uptake values were achieved by several authors testing 100 ppm of synthetic lead solutions. For example, *Carvalheiras* et al. achieved an uptake of 14 mg/g testing metakaolin/red mud-derived geopolymer

Table 3
– Comparison of magnetisation (M) values for different magnetic geopolymers.

Material	M (A m^2 kg^{-1})	Reference
Pure magnetite	90	(Ben-Arfa et al., 2019; Cornell and Schwertmann, 2006)
Copper slag geopolymer (powder)	5.60	Mullaimalar et al. (2024)
Geopolymer spheres after thermal treatment at 600 °C (bulk)	5.34	This study
Fly-ash based geopolymer/γ-Fe_2O_3 (powder)	4.95	El-Naggar et al. (2024)
Geopolymer/Fe_3O_4 nanocomposite (powder)	4.71	Khan et al. (2023)
Magnetite/geopolymer composite (powder)	3.70	(Al-husseiny and Ebrahim, 2022a, 2022b)
Geopolymer/$BaFe_{12}O_{19}$ nanocomposite (powder)	2.82	Phokha et al. (2023)
Geopolymer/Fe_3O_4 composite (powder)	2.50	Rossatto et al. (2020)
Calcined fly-ash based geopolymer (400 °C)	2.25	Payakaniti et al. (2020)
Floral magnetic sodalite microspheres (bulk)	0.52	Su et al. (2023)
Geopolymer spheres without thermal treatment (bulk)	0.15	This study

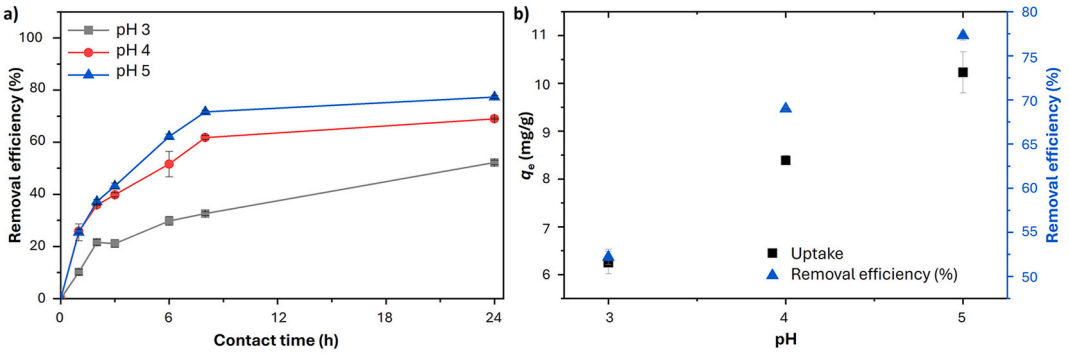

Fig. 10. – Removal efficiency over time (a) and uptake at 24 h of Pb in synthetic wastewater in function of pH (b).

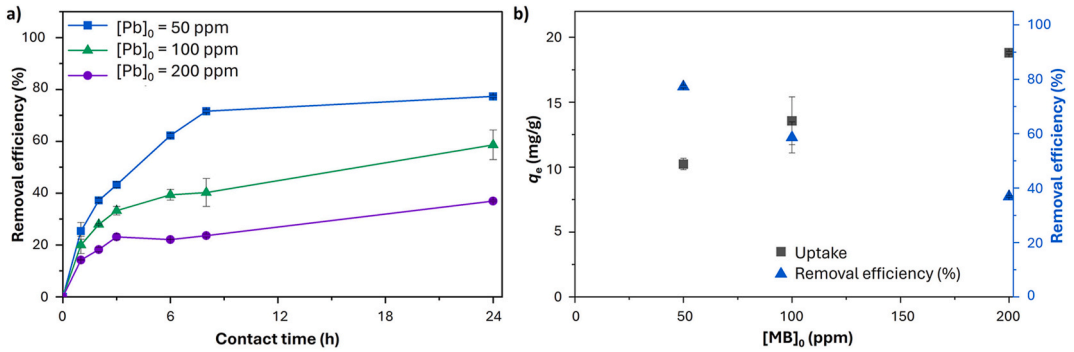

Fig. 11. – Pb removal efficiency over contact time (a) and uptake (b) in synthetic wastewater as a function of initial heavy metal concentration.

monoliths (Carvalheiras et al., 2023), *Caetano* et al. achieved 16 mg/g testing cubic fly-ash based geopolymer foams (Caetano et al., 2022) and *Novais* et al. achieved 16 mg/g testing inorganic polymer foams (Novais et al., 2020). Nevertheless, the approach explored here offers the advantage of easy and inexpensive sorbent recovery after the treatment by the use of inexpensive permanent magnets.

Metal cations, such as lead, are adsorbed onto the negatively charged aluminosilicate network of geopolymers through two primary mechanisms: physisorption and chemisorption (Saleh, 2022). Physisorption involves weak van der Waals interactions between the metal ions and the geopolymer surface, while chemisorption involves the formation of stronger chemical bonds, which can occur via ion exchange, hydrolysis, or complexation (Hijazi et al., 2024). Understanding these mechanisms is essential for optimising geopolymer-based adsorbents for wastewater treatment. Recent review papers suggest that the main sorption mechanism when using geopolymeric materials is by ion exchange (Luukkonen et al., 2019; Novais and Labrincha, 2022). Ion exchange occurs when metal ions in solution replace Na/K ions within the anionic framework of the adsorbent (-Si-O-Al-O-Si-O-). This is further corroborated by the feasibility of desorbing the Pb^{2+} ions by using acidic desorption agents (e.g., HNO_3) allowing to use the sorbents in multiple sorption cycles (Carvalheiras et al., 2023; Novais et al., 2020). The lead extraction mechanics by the magnetic geopolymer spheres is expected to be governed by ion exchange similar to what we have observed when using non-magnetic geopolymer spheres (Gonçalves et al., 2024a). This topic will be considered in future work.

3.3.3. *Feasibility of magnetic geopolymer spheres as adsorbent materials*

The use of waste as raw materials in the production of new adsorbents is an environmentally friendly and sustainable approach that contributes to the valorisation of industrial streams with no market value. Fly ash from biomass combustion can be used as an aluminosilicate source to produce geopolymers, and this has the potential to reduce the need for landfill disposal, thus reducing the impact on the surrounding habitats and ecosystems (Gameiro et al., 2021). Red mud, a by-product of alkaline treatment for aluminium production from bauxite ore, is difficult to discard due to its high alkalinity and the presence of some hazardous elements (Yang et al., 2024). This waste can also be used as an aluminosilicate source in geopolymer production, thus reducing the use of virgin raw materials, such as metakaolin, in the manufacture of these alkali-activated materials.

In recent years, geopolymers have been studied as adsorbents in the treatment of contaminated wastewaters due to their properties (chemical composition, porosity, density and specific surface area) (Caetano et al., 2022; Novais et al., 2016b, 2020). The production and use of magnetic geopolymers is a recent field of study (El-Naggar et al., 2024), and has the potential to be cost-effective compared to the chemical synthesis of magnetic nanomaterials, a widely studied and used technology to remove pollutants (Shen et al., 2023). The adsorption performance and the enhanced characteristics (magnetic properties, control of particle size and shape, crystal structure) of magnetic iron-based nanomaterials such as nano zerovalent iron (nZVI), maghemite (γ-Fe_2O_3), and magnetite (Fe_3O_4), are advantageous for several environmental and high-performance applications, such as medical imaging or high-density data storage (Qu et al., 2013). However, magnetic geopolymers are advantageous from a sustainability point-of-view, using mainly wastes in their production and exhibiting good performance for the removal of pollutants.

4. Conclusions

Red mud/fly ash-based magnetic geopolymer spheres were successfully produced through the suspension-solidification method and subsequent modification at high temperatures under N_2 by reducing the hematite contained in the red mud residue into magnetite. The geopolymer spheres, treated at 600 °C for 2 h in a reductive N_2 atmosphere, present promising magnetic properties, reaching a saturation magnetisation of 5.34 A m^2 kg^{-1}, which is a slightly higher value than those

reported by other authors for magnetic geopolymers, and in this case without the addition of any extra iron compounds to the original waste material. The feasibility of these sustainable magnetic materials as metal sorbents for polluted waters was assessed for the removal of lead, a common water contaminant. The observed uptake value of 19 mg/g demonstrates the potential of these materials for environmental applications. The production of waste-based geopolymer spheres has an economic advantage due to the use of fewer virgin raw materials during manufacturing, with magnetic properties allowing magnetic separation using inexpensive permanent magnets for the recovery of the adsorbent material after the adsorption process.

CRediT authorship contribution statement

Tânia Gameiro: Writing – original draft, Software, Methodology, Investigation, Formal analysis, Data curation. **João Carvalheiras:** Writing – original draft, Software, Methodology. **Nuno P.F. Gonçalves:** Writing – original draft, Software, Methodology. **João S. Amaral:** Writing – review & editing, Validation, Methodology. **Robert C. Pullar:** Writing – review & editing, Visualization, Validation, Formal analysis, Conceptualization. **João A. Labrincha:** Writing – review & editing, Validation, Supervision, Resources, Funding acquisition. **Rui M. Novais:** Writing – review & editing, Visualization, Validation, Supervision, Resources, Project administration, Funding acquisition, Formal analysis, Data curation, Conceptualization.

Declaration of competing interest

The authors declare that they have no known competing financial interests or personal relationships that could have appeared to influence the work reported in this paper.

Acknowledgements

This work was developed within the scope of the project CICECO-Aveiro Institute of Materials, UIDB/50011/2020 (DOI 10.54499/UIDB/50011/2020), UIDP/50011/2020 (DOI 10.54499/UIDP/50011/2020) & LA/P/0006/2020 (DOI 10.54499/LA/P/0006/2020), financed by national funds through the FCT/MCTES (PIDDAC). The authors would like to thank FCT project MAXIMUM (PTDC-CTM-CTM-2205-2020, DOI 10.54499/PTDC/CTM-CTM/2205/2020). NG acknowledges the funding from the European Union's Horizon Europe research and innovation programme under the Marie Skłodowska-Curie Actions PF grant agreement No 101065059.

Data availability

Data will be made available on request.

References

Ahmad, R., Abdullah, M.M.A.B., Ibrahim, W.M.W., Hussin, K., Ahmad Zaidi, F.H., Chaiprapa, J., Wysłocki, J.J., Błoch, K., Nabiałek, M., 2021. Role of sintering temperature in production of nepheline ceramics-based geopolymer with addition of ultra-high molecular weight polyethylene. Materials 14, 1077. https://doi.org/10.3390/ma14051077.

Al-husseiny, R.A., Ebrahim, S.E., 2022a. Effective removal of methylene blue from wastewater using magnetite/geopolymer composite: synthesis, characterization and column adsorption study. Inorg. Chem. Commun. 139, 109318. https://doi.org/10.1016/j.inoche.2022.109318.

Al-husseiny, R.A., Ebrahim, S.E., 2022b. Synthesis of nano-magnetite and magnetite/synthetic geopolymer nano-porous composite for application as a novel adsorbent. Environ. Nanotechnology, Monit. Manag. 18, 100700. https://doi.org/10.1016/j.enmm.2022.100700.

Alves, Z., Senff, L., Sakkas, K., Yakoumis, I., Labrincha, J.A., Novais, R.M., 2024. Synthesis of geopolymer composites using bauxite residue-based spheres as aggregate: novel and eco-friendly strategy to produce lightweight building materials. Cem. Concr. Compos. 148, 105478. https://doi.org/10.1016/j.cemconcomp.2024.105478.

Ben-Arfa, B.A.E., Mohseni, F., Miranda Salvado, I.M., Ferreira, J.F., Amaral, J.S., Pullar, R.C., 2019. Octylamine as a novel fuel for the preparation of magnetic iron oxide particles by an aqueous auto–ignition method. J. Alloys Compd. 805, 545–550. https://doi.org/10.1016/j.jallcom.2019.07.110.

Brandão, D.S., de Souza, F.G., Maranhão, F. da S., Pal, K., de Paula Pereira, M.C., Torres, A.C., Silva, G.B., Peçanha, T. do N., e Silva, S.E.C., Carelo, J.C., Middea, A., 2024. Biodiesel synthesis using magnetizable geopolymer as heterogeneous catalysts nanocomposite assisted by artificial intelligence. Top. Catal. 67, 785–809. https://doi.org/10.1007/s11244-024-01929-5.

Caetano, A.P.F., Carvalheiras, J., Senff, L., Seabra, M.P., Pullar, R.C., Labrincha, J.A., Novais, R.M., 2022. Unravelling the affinity of alkali-activated fly ash cubic foams towards heavy metals sorption. Materials 15. https://doi.org/10.3390/ma15041453.

Carvalheiras, J., Novais, R.M., Labrincha, J.A., 2023. Metakaolin/red mud-derived geopolymer monoliths: novel bulk-type sorbents for lead removal from wastewaters. Appl. Clay Sci. 232. https://doi.org/10.1016/j.clay.2022.106770.

Chen, Z., Zeilstra, C., van der Stel, J., Sietsma, J., Yang, Y., 2020. Review and data evaluation for high-temperature reduction of iron oxide particles in suspension. Ironmak. Steelmak. 47, 741–747. https://doi.org/10.1080/03019233.2019.1589755.

Cornell, R.M., Schwertmann, U., 2006. The Iron Oxides: Structure, Properties, Reactions, Occurrences and Uses, second ed. Wiley-VCH, Weinheim, Germany.

El-Naggar, M.R., Dong, Y., Hamed, M.M., Abd, A. El, Ibrahiem, H.H., Gouda, M.M., Mansy, M.S., Hassan, A.M.A., Abdel Rahman, R.O., 2024. Microstructural insights of magnetic γ-Fe2O3/geopolymer nanocomposite for prospective green removal of heavy metals from aqueous solutions. Sep. Purif. Technol. 333, 125941. https://doi.org/10.1016/j.seppur.2023.125941.

Franchin, G., Pesonen, J., Luukkonen, T., Bai, C., Scanferla, P., Botti, R., Carturan, S., Innocentini, M., Colombo, P., 2020. Removal of ammonium from wastewater with geopolymer sorbents fabricated via additive manufacturing. Mater. Des. 195, 109006. https://doi.org/10.1016/j.matdes.2020.109006.

Gameiro, T., Costa, C., Labrincha, J.A., Novais, R.M., 2023. Reusing spent fluid catalytic cracking catalyst as an adsorbent in wastewater treatment applications. Mater. Today Sustain. 24, 100555. https://doi.org/10.1016/j.mtsust.2023.100555.

Gameiro, T., Novais, R.M., Correia, C.L., Carvalheiras, J., Seabra, M.P., Tarelho, L.A.C., Labrincha, J.A., Capela, I., 2021. Role of waste-based geopolymer spheres addition for pH control and efficiency enhancement of anaerobic digestion process. Bioprocess Biosyst. Eng. 44, 1167–1183. https://doi.org/10.1007/s00449-021-02522-w.

Gonçalves, N.P.F., Almeida, M.M., Labrincha, J.A., Novais, R.M., 2024a. Effective acid mine drainage remediation in fixed bed column using porous red mud/fly ash-containing geopolymer spheres. Sci. Total Environ. 940, 173633. https://doi.org/10.1016/j.scitotenv.2024.173633.

Gonçalves, N.P.F., da Silva, E.F., Tarelho, L.A.C., Labrincha, J.A., Novais, R.M., 2024b. Simultaneous removal of multiple metal(loid)s and neutralization of acid mine drainage using 3D-printed bauxite-containing geopolymers. J. Hazard Mater. 462, 132718. https://doi.org/10.1016/j.jhazmat.2023.132718.

Gonçalves, N.P.F., Olhero, S.M., Labrincha, J.A., Novais, R.M., 2023. 3D-printed red mud/metakaolin-based geopolymers as water pollutant sorbents of methylene blue. J. Clean. Prod. 383, 135315. https://doi.org/10.1016/j.jclepro.2022.135315.

Hijazi, D.A., BiBi, A., Al-Ghouti, M.A., 2024. Sustainable waste utilization: geopolymeric fly ash waste as an effective phenol adsorbent for environmental remediation. Resour. Environ. Sustain. 15, 100142. https://doi.org/10.1016/j.resenv.2023.100142.

Karunadasa, K.S.P., Manoratne, C.H., Pitawala, H.M.T.G.A., Rajapakse, R.M.G., 2019. Thermal decomposition of calcium carbonate (calcite polymorph) as examined by in-situ high-temperature X-ray powder diffraction. J. Phys. Chem. Solids 134, 21–28. https://doi.org/10.1016/j.jpcs.2019.05.023.

Khan, H., Hussain, S., Zahoor, R., Arshad, M., Umar, M., Marwat, M.A., Khan, A., Khan, J. R., Haleem, M.A., 2023. Novel modeling and optimization framework for Navy Blue adsorption onto eco-friendly magnetic geopolymer composite. Environ. Res. 216, 114346. https://doi.org/10.1016/j.envres.2022.114346.

Kljajević, L., Nenadović, M., Ivanović, M., Bučevac, D., Mirković, M., Mladenović Nikolić, N., Nenadović, S., 2022. Heat treatment of geopolymer samples obtained by varying concentration of sodium hydroxide as constituent of alkali activator. Gels 8, 333. https://doi.org/10.3390/gels8060333.

Kljajević, L.M., Nenadović, S.S., Nenadović, M.T., Bundaleski, N.K., Todorović, B.Ž., Pavlović, V.B., Rakočević, Z.L., 2017. Structural and chemical properties of thermally treated geopolymer samples. Ceram. Int. 43, 6700–6708. https://doi.org/10.1016/j.ceramint.2017.02.066.

Kuenzel, C., Grover, L.M., Vandeperre, L., Boccaccini, A.R., Cheeseman, C.R., 2013. Production of nepheline/quartz ceramics from geopolymer mortars. J. Eur. Ceram. Soc. 33, 251–258. https://doi.org/10.1016/j.jeurceramsoc.2012.08.022.

Kumar, A., Saravanan, T.J., Bisht, K., Kabeer, K.I.S.A., 2021. A review on the utilization of red mud for the production of geopolymer and alkali activated concrete. Constr. Build. Mater. 302, 124170. https://doi.org/10.1016/j.conbuildmat.2021.124170.

Luukkonen, T., 2022. Surface chemistry of alkali-activated materials and how to modify it. In: Alkali-Activated Materials in Environmental Technology Applications. Elsevier, pp. 113–140. https://doi.org/10.1016/B978-0-323-88438-9.00002-8.

Luukkonen, T., Heponiemi, A., Runtti, H., Pesonen, J., Yliniemi, J., Lassi, U., 2019. Application of alkali-activated materials for water and wastewater treatment: a review. Rev. Environ. Sci. Biotechnol. 18, 271–297. https://doi.org/10.1007/s11157-019-09494-0.

Luukkonen, T., Yliniemi, J., Sreenivasan, H., Ohenoja, K., Finnilä, M., Franchin, G., Colombo, P., 2020. Ag- or Cu-modified geopolymer filters for water treatment

manufactured by 3D printing, direct foaming, or granulation. Sci. Rep. 10, 7233. https://doi.org/10.1038/s41598-020-64228-5.
Maleki, A., Hajizadeh, Z., Sharifi, V., Emdadi, Z., 2019. A green, porous and eco-friendly magnetic geopolymer adsorbent for heavy metals removal from aqueous solutions. J. Clean. Prod. 215, 1233–1245. https://doi.org/10.1016/j.jclepro.2019.01.084.
Moutaoukil, G., Sobrados, I., Alehyen, S., Taibi, M., 2024. Understanding the thermomechanical behavior of geopolymer foams: influence of rate and type of foaming agent and stabilizer. Chem. Data Collect. 50, 101111. https://doi.org/10.1016/j.cdc.2023.101111.
Mullaimalar, A., Thanigaiselvan, R., Karuppaiyan, J., Kiruthika, S., Jeyalakshmi, R., Albeshr, M.F., 2024. An efficient eco-friendly adsorbent material based on waste copper slag-biomass ash geopolymer: dye sorption capacity and sustainable properties. Environ. Geochem. Health 46, 110. https://doi.org/10.1007/s10653-024-01920-9.
Novais, R.M., Buruberri, L.H., Seabra, M.P., Bajare, D., Labrincha, J.A., 2016a. Novel porous fly ash-containing geopolymers for pH buffering applications. J. Clean. Prod. 124, 395–404. https://doi.org/10.1016/j.jclepro.2016.02.114.
Novais, R.M., Buruberri, L.H., Seabra, M.P., Labrincha, J.A., 2016b. Novel porous fly-ash containing geopolymer monoliths for lead adsorption from wastewaters. J. Hazard Mater. 318, 631–640. https://doi.org/10.1016/j.jhazmat.2016.07.059.
Novais, R.M., Carvalheiras, J., Seabra, M.P., Pullar, R.C., Labrincha, J.A., 2020. Highly efficient lead extraction from aqueous solutions using inorganic polymer foams derived from biomass fly ash and metakaolin. J. Environ. Manage. 272. https://doi.org/10.1016/j.jenvman.2020.111049.
Novais, R.M., Labrincha, J.A., 2022. Alkali-activated materials as adsorbents for water and wastewater treatment. In: Luukkonen, T. (Ed.), Alkali-Activated Materials in Environmental Technology Applications. Elsevier, Kidlington, United Kingdom, pp. 143–166. https://doi.org/10.1016/B978-0-323-88438-9.00003-X.
Padilla, I., López-Delgado, A., Romero, M., 2022. Kinetic study of the transformation of sodalite to nepheline. J. Am. Ceram. Soc. 105, 4336–4347. https://doi.org/10.1111/jace.18365.
Payakaniti, P., Chuewangkam, N., Yensano, R., Pinitsoontorn, S., Chindaprasirt, P., 2020. Changes in compressive strength, microstructure and magnetic properties of a high-calcium fly ash geopolymer subjected to high temperatures. Constr. Build. Mater. 265, 120650. https://doi.org/10.1016/j.conbuildmat.2020.120650.
Phokha, S., Boonserm, K., Chirawatkul, P., Chanlek, N., Kidkhunthod, P., Sata, V., Chindaprasirt, P., Hunpratub, S., 2023. Investigation of the magnetic and mechanical performance of fly ash Geopolymer/BaFe12O19 nanocomposites. Radiat. Phys. Chem. 209, 110995. https://doi.org/10.1016/j.radphyschem.2023.110995.
Pineau, A., Kanari, N., Gaballah, I., 2006. Kinetics of reduction of iron oxides by H2: Part I: low temperature reduction of hematite. Thermochim. Acta 447, 89–100. https://doi.org/10.1016/j.tca.2005.10.004.
Pulidori, E., Pelosi, C., Fugazzotto, M., Pizzimenti, S., Carosi, M.R., Bernazzani, L., Stroscio, A., Tiné, M.R., Mazzoleni, P., Barone, G., Duce, C., 2024. Thermal behavior of Sicilian clay-based geopolymers. J. Therm. Anal. Calorim. https://doi.org/10.1007/s10973-024-13226-0.
Qu, X., Alvarez, P.J.J., Li, Q., 2013. Applications of nanotechnology in water and wastewater treatment. Water Res. 47, 3931–3946. https://doi.org/10.1016/j.watres.2012.09.058.
Riyanto, A., Sembiring, S., Husain, S., Karimah, R.S., Firdaus, I., 2021. Rietveld analysis of geopolymer prepared from amorphous rice husk silica with different thermal treatment. J. Phys. Conf. Ser. 1751, 012070. https://doi.org/10.1088/1742-6596/1751/1/012070.
Rossatto, D.L., Netto, M.S., Jahn, S.L., Mallmann, E.S., Dotto, G.L., Foletto, E.L., 2020. Highly efficient adsorption performance of a novel magnetic geopolymer/Fe3O4 composite towards removal of aqueous acid green 16 dye. J. Environ. Chem. Eng. 8, 103804. https://doi.org/10.1016/j.jece.2020.103804.
Salah, A.M., Selim, A.Q., Yehia, A., Bonilla-Petriciolet, A., Seliem, M.K., Ali, R.A.M., 2024. A novel magnetic geopolymer-based adsorbent prepared from heated glauconite and separated magnetite: experiments and statistical physics treatment for crystal violet. Sep. Purif. Technol. 342, 126942. https://doi.org/10.1016/j.seppur.2024.126942.
Saleh, T.A., 2022. Adsorption technology and surface science. In: Interface Science and Technology, pp. 39–64. https://doi.org/10.1016/B978-0-12-849876-7.00006-3.
Shen, Z., Kuang, Y., Zhou, S., Zheng, J., Ouyang, G., 2023. Preparation of magnetic adsorbent and its adsorption removal of pollutants: an overview. TrAC Trends Anal. Chem. 167, 117241. https://doi.org/10.1016/j.trac.2023.117241.
Singh, J., Singh, S.P., 2019. Geopolymerization of solid waste of non-ferrous metallurgy – a review. J. Environ. Manage. 251, 109571. https://doi.org/10.1016/j.jenvman.2019.109571.
Stoicescu, C.S., Culita, D., Stanica, N., Papa, F., State, R.N., Munteanu, G., 2022. Temperature programmed reduction of a core-shell synthetic magnetite: dependence on the heating rate of the reduction mechanism. Thermochim. Acta 709, 179146. https://doi.org/10.1016/j.tca.2022.179146.
Su, Q., He, Y., Yang, S., Wan, H., Chang, S., Cui, X., 2021. Synthesis of NaA-zeolite microspheres by conversion of geopolymer and their performance of Pb (II) removal. Appl. Clay Sci. 200, 105914. https://doi.org/10.1016/j.clay.2020.105914.
Su, Q., Wei, X., Yang, G., Ou, Z., Zhou, Z., Huang, R., Shi, C., 2023. In-situ conversion of geopolymer into novel floral magnetic sodalite microspheres for efficient removal of Cd(II) from water. J. Hazard Mater. 453, 131363. https://doi.org/10.1016/j.jhazmat.2023.131363.
Tan, T.H., Mo, K.H., Ling, T.-C., Lai, S.H., 2020. Current development of geopolymer as alternative adsorbent for heavy metal removal. Environ. Technol. Innov. 18, 100684. https://doi.org/10.1016/j.eti.2020.100684.
Tchakouté, H.K., Rüscher, C.H., Kong, S., Kamseu, E., Leonelli, C., 2017. Thermal behavior of metakaolin-based geopolymer cements using sodium waterglass from rice husk ash and waste glass as alternative activators. Waste and Biomass Valorization 8, 573–584. https://doi.org/10.1007/s12649-016-9653-7.
Yang, M., Chen, L., Lai, J., Osman, A.I., Farghali, M., Rooney, D.W., Yap, P.-S., 2024. Advancing environmental sustainability in construction through innovative low-carbon, high-performance cement-based composites: a review. Mater. Today Sustain. 26, 100712. https://doi.org/10.1016/j.mtsust.2024.100712.
Zawrah, M.F., Sadek, H.E.H., Ngida, R.E.A., Sawan, S.E.A., El-Kheshen, A.A., 2022. Effect of low-rate firing on physico-mechanical properties of unfoamed and foamed geopolymers prepared from waste clays. Ceram. Int. 48, 11330–11337. https://doi.org/10.1016/j.ceramint.2021.12.356.